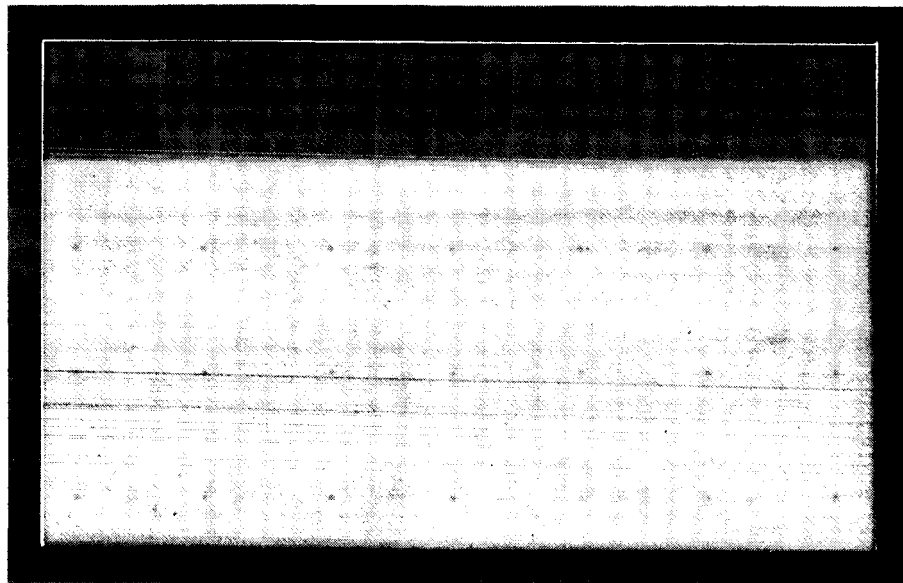
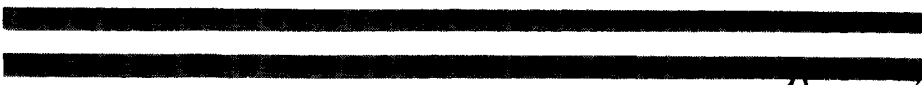
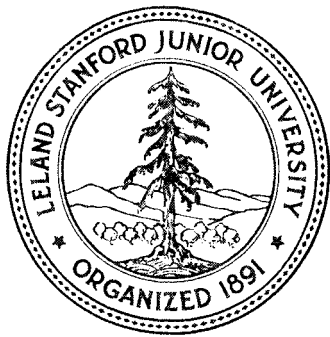


111111-1111 111111

12-29

11339

P-28



(NASA-CR-180602) PROTEIN CRYSTAL GROWTH IN
LCW GRAVITY Annual Technical Report, 1 Jan.
- 31 Dec. 1986 (Stanford Univ.) 28 p
Avail: NTIS HC A03/MF A01 CSDL 20B

N87-22059

Unclas
G3/29 0071339

CENTER FOR MATERIALS RESEARCH

STANFORD UNIVERSITY • STANFORD, CALIFORNIA

The Board of Trustees of the
Leland Stanford Junior University
Center for Materials Research
Stanford, CA 94305
Santa Clara, 12th Congressional District

Annual Technical Report

PROTEIN CRYSTAL GROWTH IN LOW GRAVITY
NAG 8-489

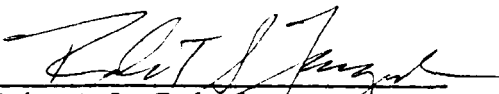
January 1, 1986 through December 31, 1986

Submitted to

National Aeronautics and Space Administration
Marshall Space Flight Center
Huntsville, Alabama 35812

CMR-87-5

Principal Investigator


Robert S. Feigelson
Professor (Research)
Center for Materials Research
Crystal Science and Engineering

May 22, 1987

TABLE OF CONTENTS

I. SOLUBILITY	3
A. Introduction	3
B. Experimental Procedures.	3
C. Results.	4
D. Discussion	7
E. Conclusions.	9
II. GROWTH RATE	10
A. Introduction	10
B. Experimental Procedures.	10
C. Results.	11
D. Discussion	14
E. Conclusions.	19
III. SCHLIEREN	19
A. Introduction	19
B. Experimental Procedures.	20
C. Results.	21
D. Discussion	21
IV. REFERENCES	25

ABSTRACT

This report covers the period from January 1 to December 31, 1986. During this period the solubility and growth mechanism of canavalin were studied, and the applicability of the Schlieren technique to protein crystal growth was investigated.

Canavalin which may be crystallized from a basic solution by the addition of hydrogen (H^+) ions was shown to have "normal" solubility characteristics over the range of temperatures (5 to 25°C) and pH (5 to 7.5) studied. The solubility data combined with growth rate data gathered from the seeded growth of canavalin crystals indicated that the growth mechanism at high supersaturation ratios (>1.28) is screw dislocation like.

A Schlieren apparatus was constructed and flow patterns were observed in Rochelle salt (sodium potassium tartrate), lysozyme, and canavalin. The critical parameters were identified as the change in density with concentration ($d\rho/dc$) and the change in index of refraction with concentration (dn/dc). Some of these values have been measured for the materials listed.

INTRODUCTION

The ultimate goal of this three-year program is the careful design of an experiment for the growth of protein crystals in a long-duration space flight. The ground-based experiments are being performed to optimize the conditions for growth in space and to provide a data base to compare against the results obtained in space in a future program. The data gathered will also provide insight into the mechanisms of protein crystal growth.

The goals of the first two years of this program were to develop equipment and techniques to study the growth of crystals in a model protein system. The data gathered during these experiments will be used to model and understand the mechanisms of protein crystal growth. It will also form the basis for comparison with data collected during long-term space flights.

During the year covered by this report (January 1 to December 31, 1986) three separate studies were conducted using the protein canavalin as a model system. Solubility and growth rate studies were undertaken in an effort to understand the mechanisms involved in the nucleation and crystal growth of proteins. Schlieren experiments were used to study fluid flow during growth. Each area will be discussed separately.

I. SOLUBILITY

A. Introduction

It is necessary to understand the solubility relationships in a crystallizing system in order to effectively control the growth process. Mullin¹ lists solubility as the first information needed for designing a crystallizing system. Coupled to the solubility is the concept of supersaturation as the driving force for isothermal crystallization. Supersaturation is expressed in terms of the solution concentration (c) and the concentration at saturation (s) and is usually given as either a difference (c-s) or a ratio (c/s). Plots of growth rate versus supersaturation can be used to determine the growth mechanism (see for example Fiddlis, et.al²). Supersaturation data can also be used to determine nucleation rate¹. Knowledge of the solubility curves also assists in planning growth experiments.

In most inorganic systems the solubility curves are relatively simple relationships between temperature and concentration of the crystallizing species. The situation in a protein system is somewhat more complex. In addition to the crystallizing species (the protein), the concentration of hydrogen ion, precipitating agents, and salts added for stabilization must be considered as well as the effect of temperature. The system we chose to study is a rather simple one consisting of the protein canavalin, water, sodium chloride (NaCl-1% by weight) added as a stabilizer³, and hydrogen ion (H⁺). The variables studied included temperature and H⁺ concentration as measured by pH.

B. Experimental Procedures

Canavalin (obtained from Alexander McPherson, University of California, Riverside) was dissolved in a water solution adjusted to pH 9.2 to 9.5 with ammonium hydroxide (NH₄OH) and containing 1% NaCl. The solution was filtered using a 1.0 μ filter followed by a 0.22 μ filter. Aliquots of this starting solution were removed and their pH adjusted to the desired initial pH using acetic acid (HAc). These solutions were placed in culture dishes and each individual compartment sealed

to the desired initial pH using acetic acid (HAc). These solutions were placed in culture dishes and each individual compartment sealed using silicon vacuum grease. The culture plates were placed in controlled temperature incubators and allowed to equilibrate for 2 weeks. At the end of this period, the pH of the solution was measured and, after filtration, the concentration of canavalin in the supernatant liquid was measured using a spectrophotometer. These experiments covered a temperature range of 5 to 25°C in 5°C increments and a pH range of 5 to 7.5 in steps of 0.5.

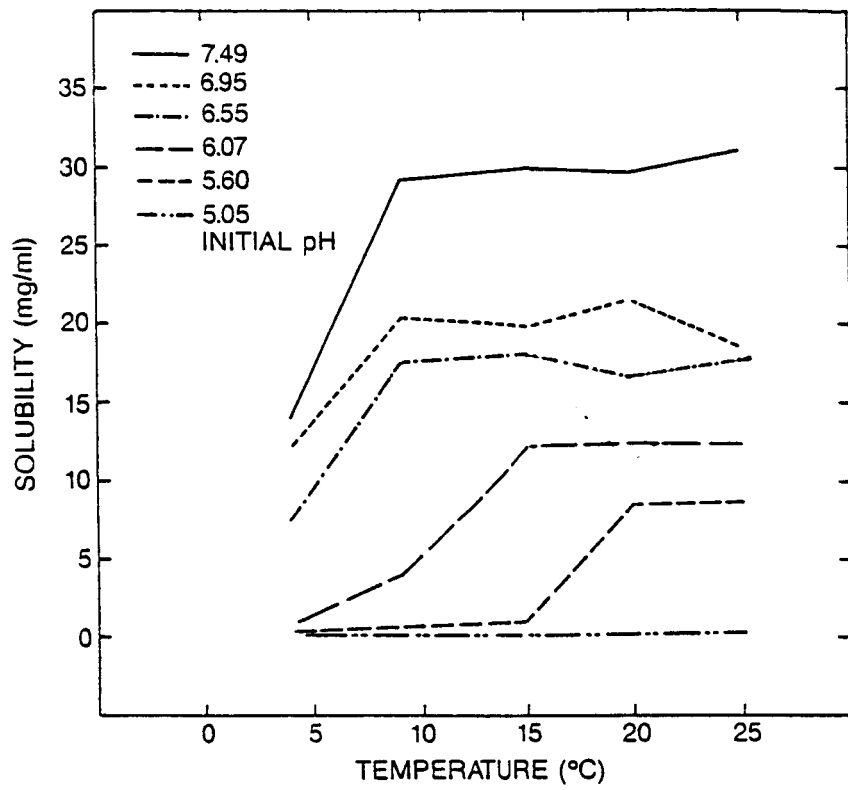
C. Results

The results of these experiments are shown in Figure 1. Figure 1a shows the temperature dependence of solubility. The solubility curves show a fairly flat solubility vs. temperature dependence at higher temperatures followed by a break which shifts to higher temperatures as the pH is lowered. It was also noted that massive spontaneous precipitation occurs at pH's lower than ~ 6.5 if the canavalin concentration is significantly above the solubility curve.

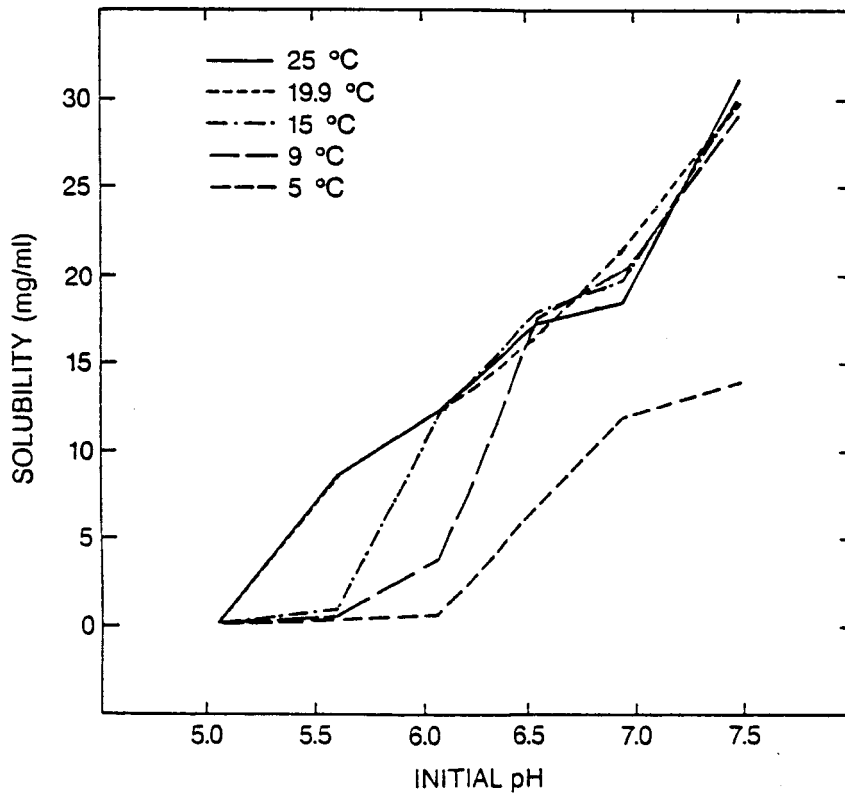
Figure 1b shows the solubility plotted against pH. The solubility decreases with decreasing pH.

Figure 2 shows the changes in pH during the solubility experiment. The final pH minus the initial pH is plotted versus initial pH and temperature. Since the systems were sealed during the equilibration period the change in pH cannot be attributed to evaporation. At 25°C (Figure 2a) with the exception of pH 5.05, the lower pH's show the largest change (increase) in pH (decrease in H⁺ concentration). As the temperature is lowered, the two lowest pH's (pH 5.05 excepted) break sharply and eventually the change becomes negative (increase in H⁺ concentration) as does pH 7.49. pH 5.05 never goes positive.

Figure 2b suggests that at a given temperature there is a pH at which the slope of the change in pH will change from positive to negative.

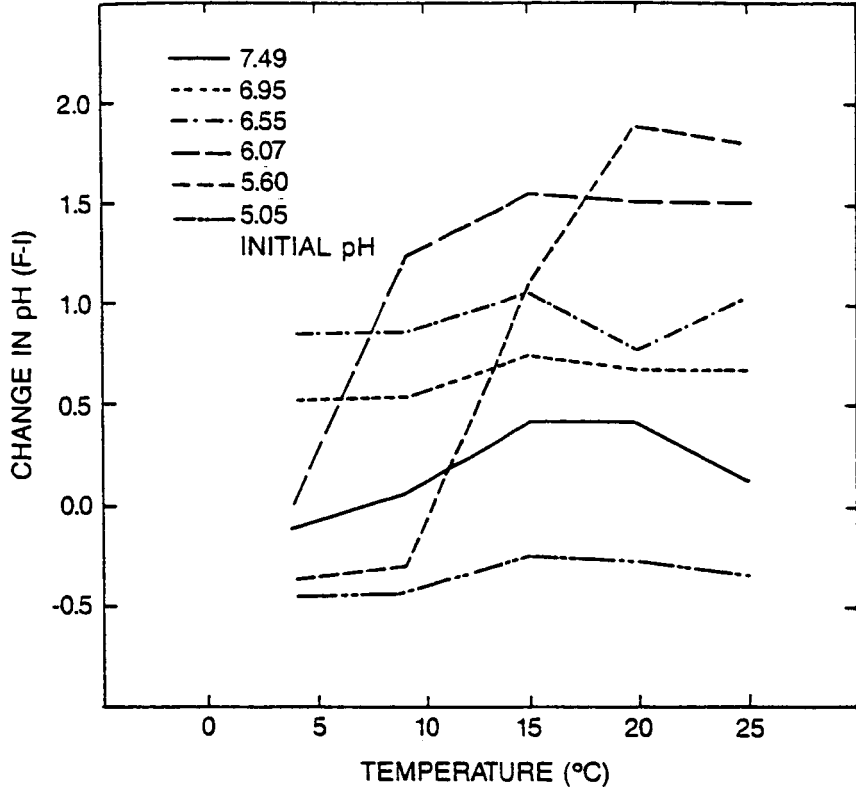


a

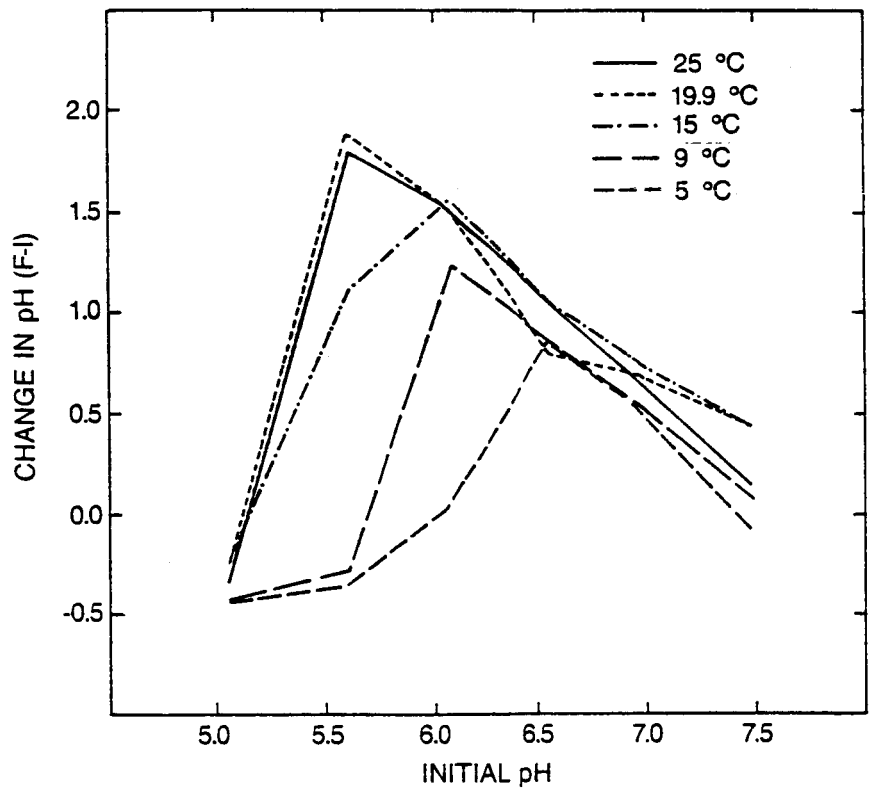


b

Figure 1: Solubility of canavalin plotted a) versus temperature at fixed initial pH, and b) versus initial pH at fixed temperature.



a



b

Figure 2: a) Change in pH (final (F) minus initial (I)) during precipitation plotted a) versus temperature at fixed initial pH, and b) versus initial pH at fixed temperature.

D. Discussion

The solubility curves of Figure 1 represent what may be classified as normal solubility behavior. An increase in the amount of the precipitating agent, in this case H^+ , causes a decrease in solubility. Likewise lowering the temperature decreases solubility. The ultimate utility of solubility curves is in predicting nucleation and growth. Figure 3 is a replot of two solubility curves with the control variable (temperature or pH) plotted on the ordinate. The driving force for either nucleation or growth is the supersaturation. In Figure 3, any point lying on an isotherm (Figure 3a) or an iso pH line (Figure 3b) and to the right of the solubility curve is in a region of supersaturation. The amount of supersaturation is given by the difference between the concentration at a point in the supersaturated region and the concentration at which an isotherm (or iso pH line) through the point crosses the solubility curve. There are actually two other curves of interest which could be placed on the diagrams: The curve of supersaturation necessary for growth and the curve of supersaturation necessary for nucleation. For any given concentration these will lie below the solubility curve. Possible growth and nucleation curves have been drawn in Figure 3a. While the growth and nucleation curves may not be known, their relationship to the solubility curve can be used to give some generalized rules for nucleation and growth. Since the differences in concentration between growth and nucleation is smaller in a steeply rising portion of the curves, nucleation should be induced in this region if possible. This will lead to less secondary nucleation or uncontrolled growth due to supersaturation than might occur in a flatter region of the curve. In the example of Figure 3a, above $10^\circ C$ the supersaturation difference along any isotherm between growth and nucleation is ~ 0.2 mg/ml; while below $5^\circ C$, it is ~ 6 mg/ml. Once nucleation has occurred or if a seeded growth technique is being used the rate of growth can be controlled by controlling the temperature. However the rate of cooling will have to be adjusted to match the slope

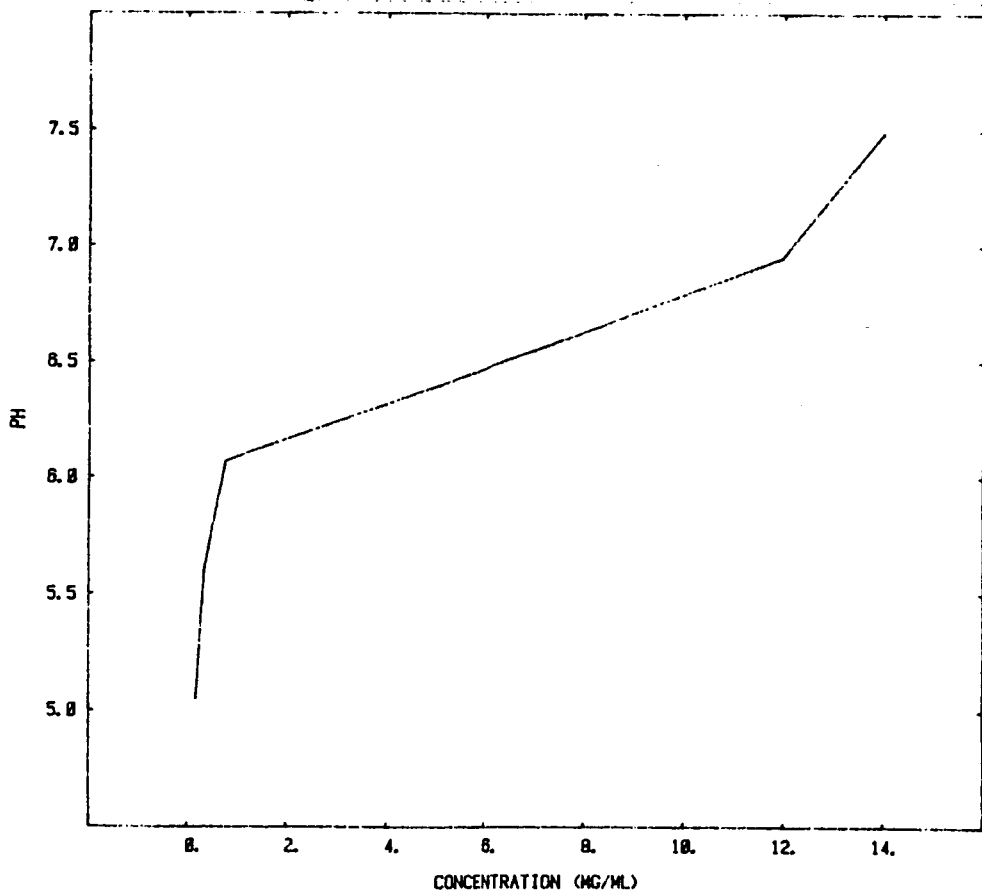
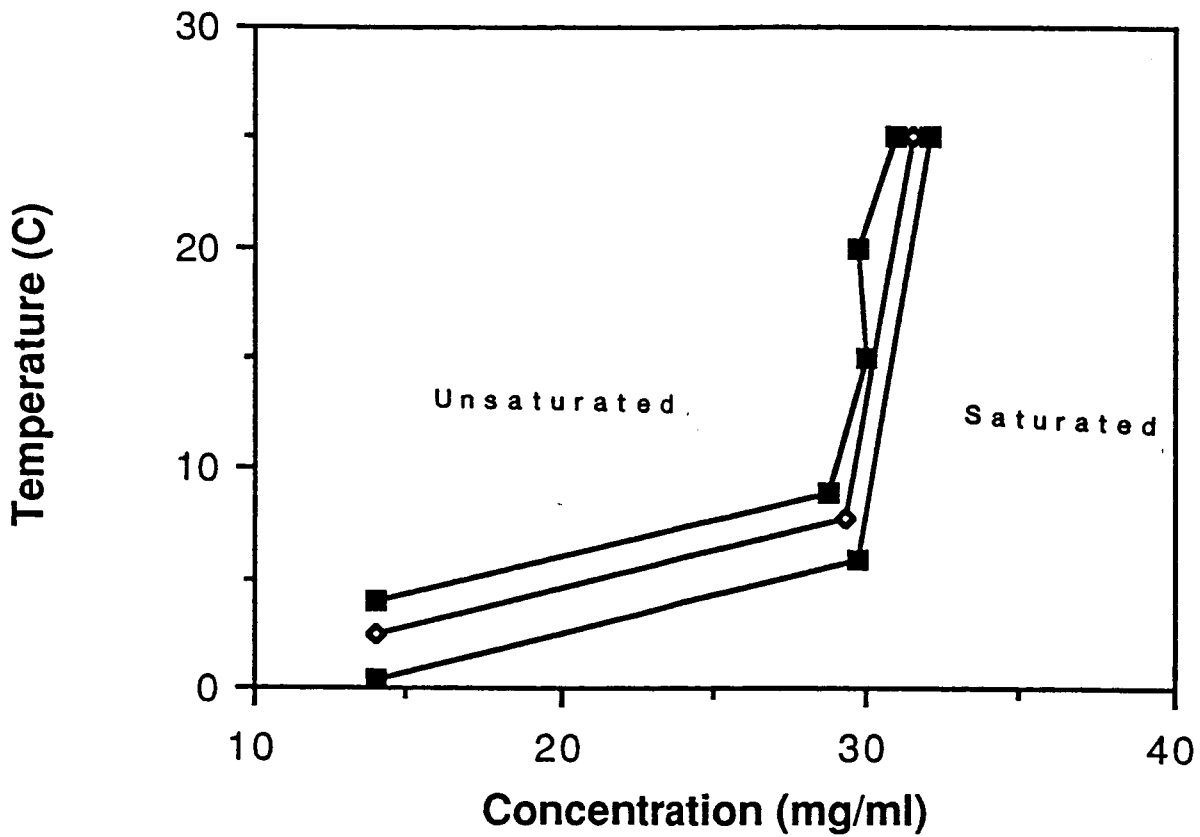


Figure 3: a) Temperature - concentration diagram at pH 7.49 with possible growth (◇) and nucleation (■) supersaturation curves plotted to the right and below the solubility curve, b) pH - concentration diagram at 4°C with solubility curve plotted.

of the growth curve to prevent rapid increases in supersaturation and the attendant possibility of uncontrolled growth in the flatter regions of the curve.

These curves may also be used to optimize the protein yield. Using the curve of Figures 3a and b, a possible scheme might be used as follows. A solution of 30 mg/ml of canavalin at 25°C and pH 7.49 is gradually cooled to 4°C. This would remove slightly more than half of the starting material. A slow increase of H⁺ concentration from pH 7.49 to pH 5.05 would remove virtually all of the remaining protein. If the protein from 1 ml of solution could be grown into a single crystal by this method, it would measure ~ 3mm on an edge. In the case of proteins which are less abundant than canavalin, following such a scheme would conserve material.

The hydrogen ion was chosen as the precipitating agent in these experiments because its concentration is easily monitored and could lead to some insight into the interaction between the protein and H⁺ during nucleation and growth. The results presented in Figure 2 confirm the fact that H⁺ ions do interact with protein molecules and in most instances are removed from the solution during crystallization (precipitation). The interaction is both pH and temperature dependent. Figure 2a shows that the protein - H⁺ ion interaction as indicated by the pH changes is strongest at lower pH's (except for pH 5.05). This interaction is temperature dependent and as temperature is decreased there is less interaction; some combinations of initial pH and temperature actually show a decrease in pH indicating a release of H⁺ ion from the protein. An initial pH of 5.05 shows this latter behavior throughout the temperature range studied. The exact cause of this behavior is not known, but McPherson³ has suggested that a different oligomeric configuration may be involved.

E. Conclusions

The following conclusions can be drawn from these results:

1. Canavalin follows a "normal" solubility behavior over the range of

temperature and pH studied (i.e. solubility decreases with decreasing temperature and with increasing precipitating agent concentration).

2. The solubility curves can be used to plan crystallization experiments by selecting optimum conditions for nucleation and/or growth.
3. The solubility curves can be used to devise experiments which will make efficient use of the material available.
4. An interaction between hydrogen ion and canavalin has been shown, but its exact nature requires more study.

II. GROWTH RATE

A. Introduction

One of the goals of this program is to study the mechanisms involved in protein crystal growth. At one level this can be the determination of how the asymmetrical unit is incorporated into the growing crystal and what the controlling factors are. In the broadest terms the rate of incorporation is controlled by either diffusion or interface kinetics. Which of these is the rate determining step can be determined by investigation of the growth rate of protein crystals versus supersaturation². In these studies canavalin was also used.

Initially the parameters affecting growth rate were identified as pH, temperature, protein concentration and salt concentration. Based on the solubility experiments described previously it appeared that while solubility was a strong function of pH, particularly at the higher pH's (above 6.0), the main effect of varying pH is to alter the solubility limit and hence the supersaturation. Initially the growth rate data is being evaluated using this premise.

B. Experimental Procedures

It is possible to do both seeded and unseeded growth rate experiments. The unseeded growth experiments, however, require a substantial amount of time for first the nucleation stage and then the growth of the nucleated crystals to a size large enough to be observed. This leads to an ambiguity in the time it takes for growth to start and the

the actual supersaturation conditions present during which growth is taking place. Therefore, all of the growth rate data was collected from seeded growth.

The growth apparatus consists of a thermostated holder which contains eight cells (.95 cm diameter x .32 cm deep). The holder is mounted on an x-y stage of a microscope which allows the growing crystals to be observed and photographed. Solutions are introduced into the cells using hypodermic syringes and needles.

The experiments are carried out in two stages: First seeds are grown in the cells using a canavalin concentration and pH which has been shown to give a small number of good crystals. The seeding solution is withdrawn from the cell and replaced with the solution whose growth rate characteristics are being studied. Selected crystals are photographed after the new solution has been added and hourly thereafter for three to four hours.

C. Results

Figure 4 shows a typical canavalin crystal grown during this phase of the program. The growth of the crystal is determined by measuring the distance between parallel edges on the crystal and converting to microns using a photograph of a precision-ruled scale. Table I shows the growth rate data gathered to date. There are two entries per crystal; one for each set of parallel edges which represent an average of the measurements. Thus four entries represent measurements on two crystals. This approach closely follows that used by Fiddis, et al.² and by Pusey and Naumann⁴ to investigate the kinetics of lysozyme growth.

The results shown in Table I are somewhat anomalous in that the crystal photographed in some instances show positive growth rates at supersaturation ratios (c/s) of less than one. This would indicate that the actual supersaturation must be higher than that calculated. In most of the growth cells there were more than the one or two

ORIGINAL PAGE IS
OF POOR QUALITY

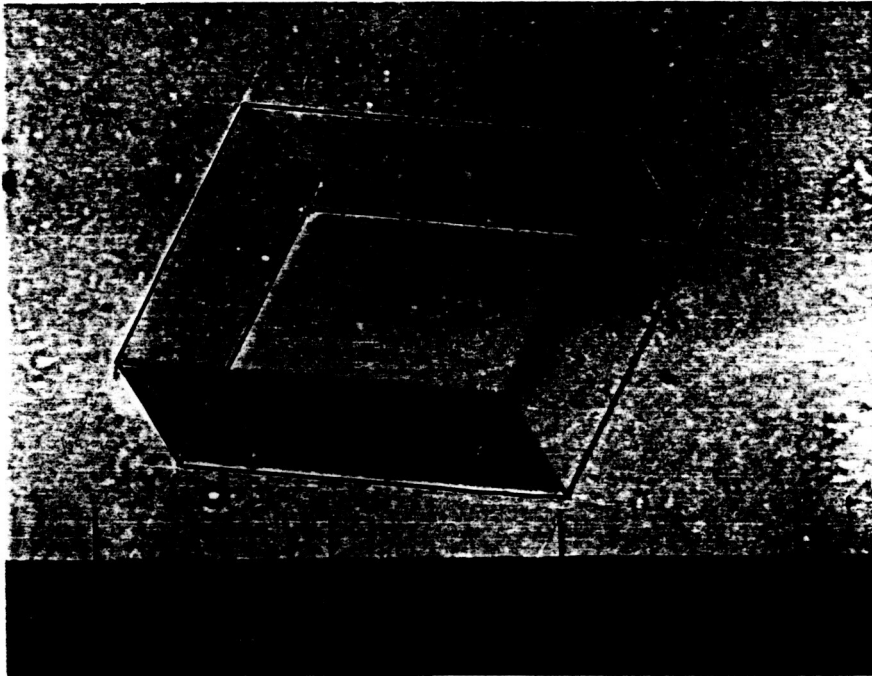


Figure 4 : Canavalin crystal grown during growth rate studies. Scale is 100 μm per division.

Table I: Growth Rate Data for Canavalin at 20°C

Protein Concentration (mg/ml)	pH	Temperature (°C)	Solubility (mg/ml)	(C-S) (mg/ml)	(C/S)	Growth Rate (μ/min)
36.10	6.99	20.8	21.57	14.53	1.67	.272 ± .022 .430 ± .041 .451 ± .034 .315 ± .010
31.60	6.97	20.8	21.24	10.36	1.49	.183 ± .017 .193 ± .020 .120 ± .011 .122 ± .020
27.99	7.01	20.8	21.92	6.07	1.28	.058 ± .021 .054 ± .007 .144 ± .046 .061 ± .024
23.23	7.00	20.8	21.71	1.52	1.07	.020 ± .007 .016 ± .012 .021 ± .024 .010 ± .049
18.63	7.02	20.3	22.27	-3.64	0.84	.010 ± .025 -.019 ± .023
12.78	6.52	20.8	17.10	-4.32	0.75	.031 ± .017 .091 ± .038 .039 ± .037 -.045 ± .067
6.39	6.54	20.8	17.10	-10.71	0.37	-.073 ± .144 -.010 ± .183 -.135 ± .079 -.050 ± .074
4.15	6.45	20.3	11.70	-7.55	0.35	.035 ± .008 .022 ± .030 .006 ± .023 .050 ± .030

crystals that were photographed. In some cases these crystals were quite small. Due to surface energy considerations, these small crystals can dissolve preferentially and some of their mass can contribute to the growth of the larger crystals. If all of the crystals were observed, there should be a net loss of crystalline mass to yield a final solution whose concentration is given by the solubility curves. Figure 5 is a plot of growth rates versus concentration for supersaturation ratios (c/s) greater than 1.0.

D. Discussion

Fiddis et al.² has presented several forms of growth rate theory based on the models discussed by Brice⁵ and Nielsen⁶. For diffusion control the growth rate takes the form

$$G = \frac{Dv(c-s)}{t} \quad (1)$$

where D is the diffusion coefficient, v the molecular volume and t the solute boundary layer (estimated by Nielsen⁶ to be 10-100 μ m). If the crystal is growing under interface kinetic control one of three models can apply. If the whole surface of the crystal is available for growth then

$$G = \frac{D}{d} vc \ln(c/s) \quad (2)$$

where d is the molectuar diameter. For growth on a screw dislocation

$$G = 0.05 D \frac{d^2}{\gamma} K T c [\ln(c/s)]^2 \quad (3)$$

where γ is the surface free energy. Finally the growth rate for spontaneous two dimensional nucleation on the surface is give by

$$G = 1.7 D d (c-s)^{2/3} \exp\left(\frac{\pi\gamma^2}{3K^2T^2\ln(c/s)}\right) \quad (4)$$

In order to decide on which growth mechanism applies to canavalin in our experiment, the growth rate data was plotted according to these various models seeking the best straight line fit. Figure 6 shows the results of the best fit. If only the points with c/s ratios of 1.28 and above are considered, the best fit is given by

$$G = 1.051 c [\ln(c/s)]^2 - .063$$

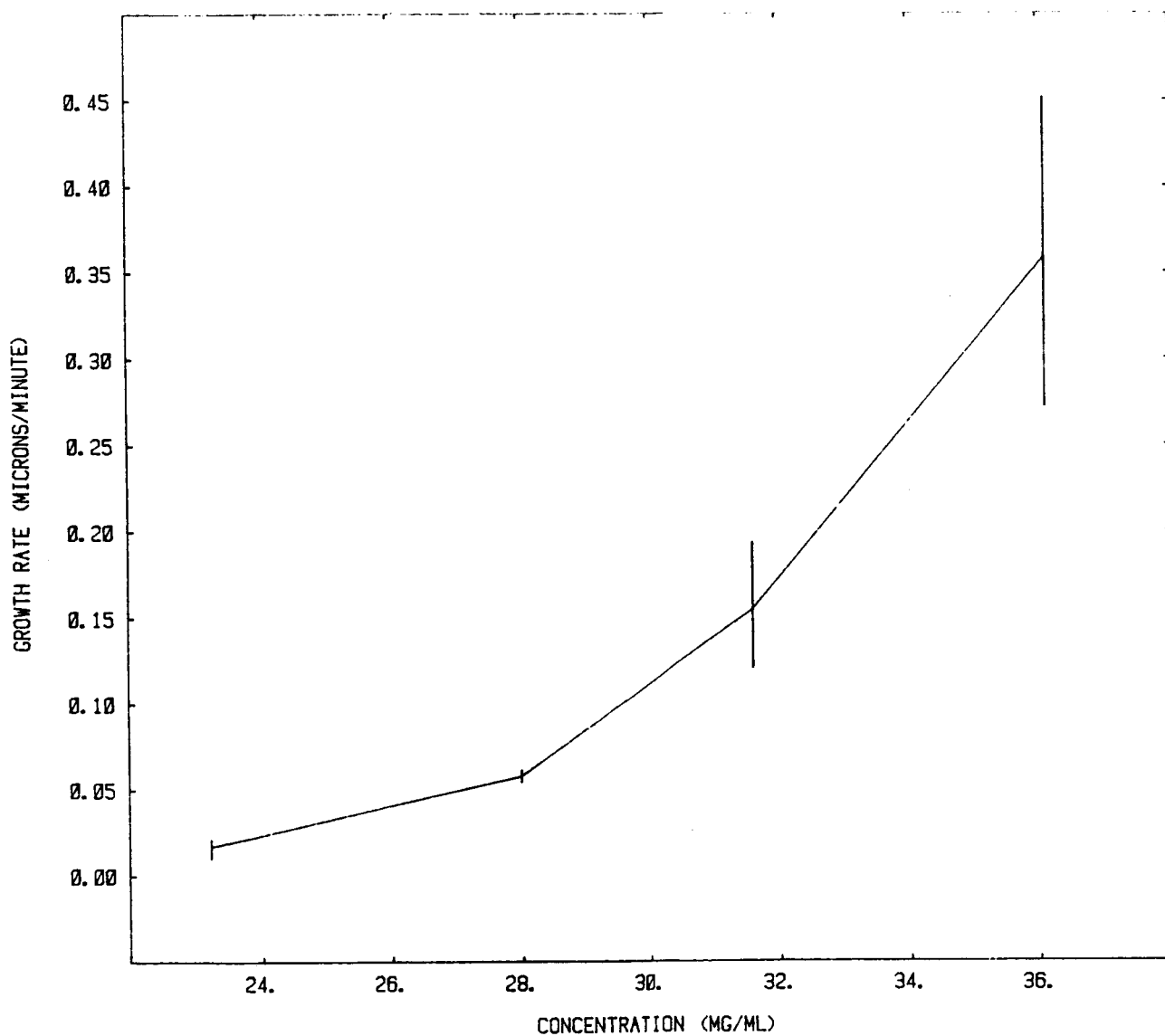


Figure 5: Growth rate versus concentration (c/s>1). Error bars indicate maximum data spread.

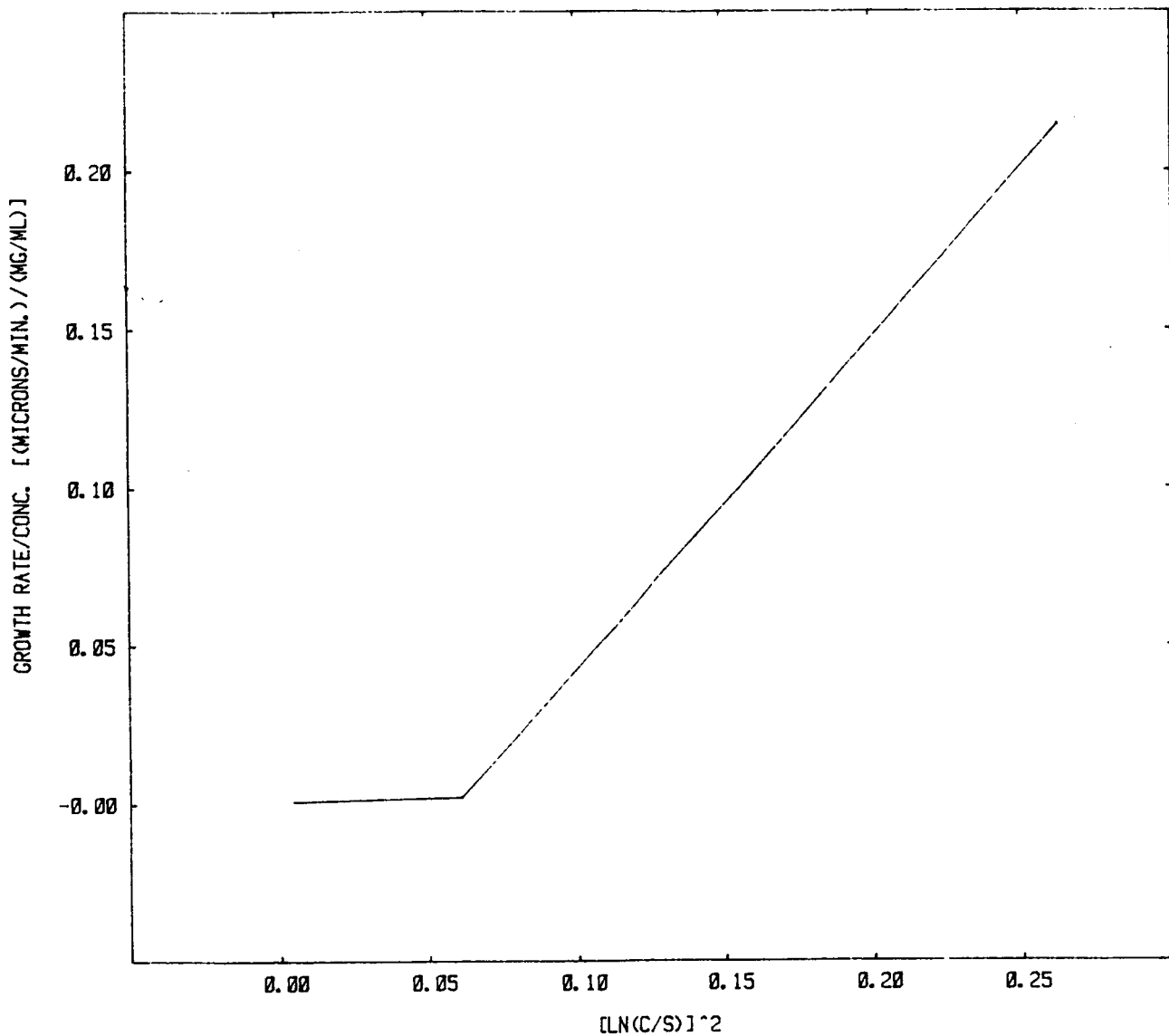


Figure 6: Plot of growth rates/concentration versus the square of the natural log of the supersaturation ratio. Upper part of the curve is fitted by $G - 1.051 c [\ln(c/s)]^{2-0.063}$.

Inclusion of all data points gives

$$G = 0.874 c [\ln(c/s)]^2 - .026$$

This fit is consistent with Equation 3 and indicative of growth on a screw dislocation. The drastic change in slope at low supersaturation ratios may be indicative of a region of diffusion limited growth. If this is the case, the growth rate in this region is given by

$$G = 0.00895 (c-s) + .00320$$

Combining Equations 1 and 3, it is then possible to make an estimate of γ .

$$\gamma = .05 \times \frac{.00895}{1.051} \frac{td^2}{v} KT$$

Using a molar volume based on the work of McPherson and Spenser⁷ and a range for t of 10 to 100 μ gives a range of values for γ from 0.9 KT to 9.0 KT. These values can be compared with the value reported by Durbin and Feher⁸ for Lysozyme (5% NaCl, $T = 24^\circ\text{C}$, $\text{pH} = 4.6$) of $\gamma_{101} = 1.9$ KT and $\gamma_{110} = 2.3$ KT, and with those of Fiddis, et al.² ($T = 20^\circ\text{C}$, $\text{pH} = 4$) of 3.1 KT and 3.9 KT.

This data can be handled in another manner. Figure 7 is a $\ln\text{-}\ln$ plot of growth rates versus (c/s) . This plot will yield the coefficients of a equation of the form

$$G = b (c/s)^m \quad (5)$$

A best fit to this curve gives

$$G = .012 (c/s)^{6.66}$$

this expression does not correspond to any of the models used to explain crystal growth. Its utility lies in its use to predict growth rates throughout the supersaturation range and thus allow the growth rate to be controlled at different conditions by combining this curve with the solubility curves.

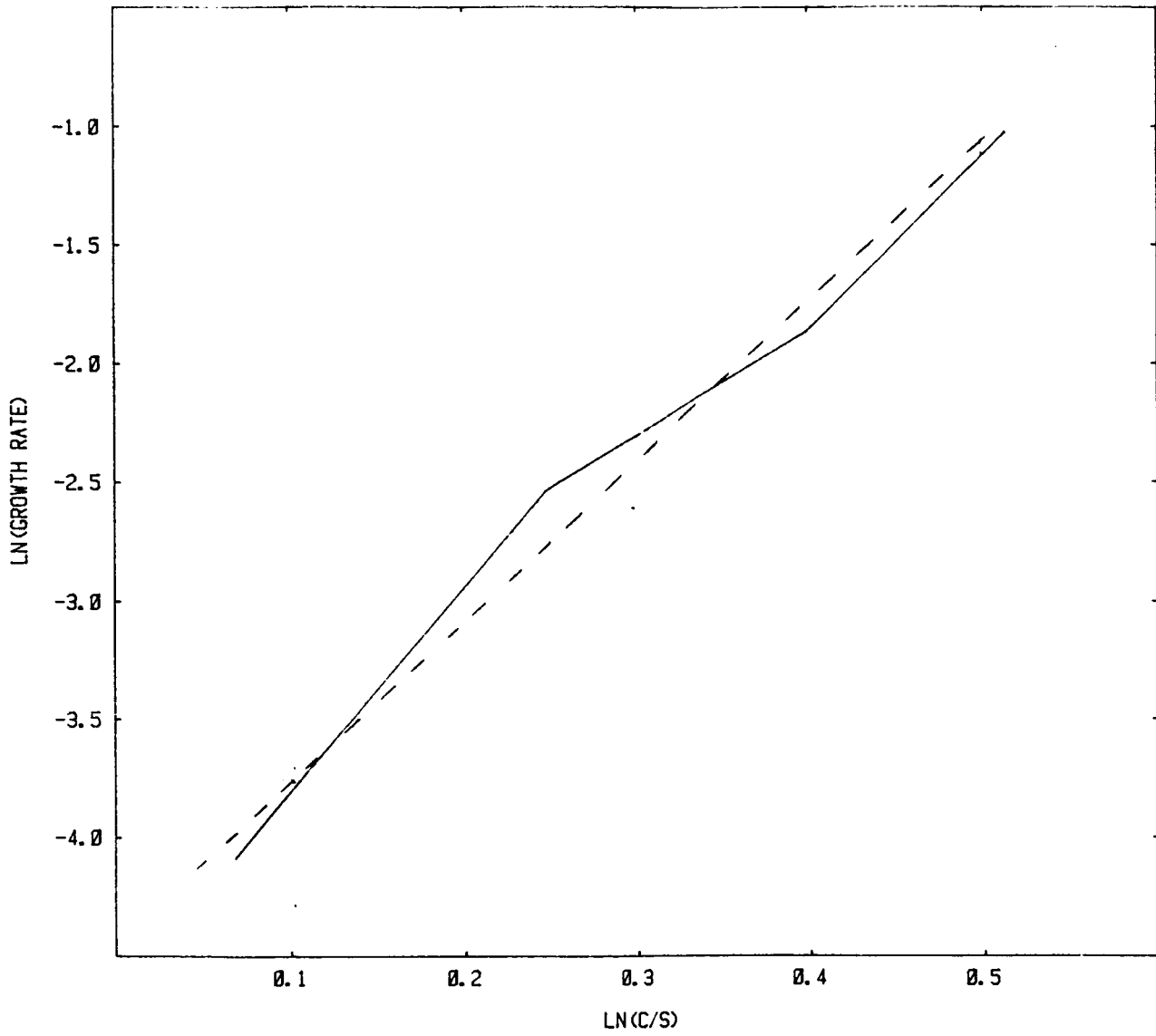


Figure 7: Plot of the natural log of the growth rate versus the natural log of the growth rate versus the natural log of the super saturation ratio. The dotted line fit is given by $G = 0.012 (c/s)^{6.66}$

E. Conclusions

The following conclusions may be drawn from this study:

1. In the supersaturation range studied there are apparently two growth regimes. At low supersaturation the growth is diffusion controlled; at higher supersaturation growth is controlled by a screw dislocation mechanism.

2. The diffusion controlled region is described by

$$G = .00895 (c-s) + .00320$$

and the kinetic controlled region by

$$G = 1.051 c [\ln (c/s)]^2 + .063$$

3. Combining the general equations for these two regions and the coefficients found by graphical analysis gives an estimate of γ in the range of 0.9 to 9.0 KT depending on the boundary layer thickness.

4. A ln-ln plot gives a predictive relationship

$$G = 0.012 (c/s)^{6.66}$$

which with the solubility curves will allow the growth rate to be adjusted under a variety of conditions.

III. SCHLIEREN

A. Introduction

One of the reasons for taking protein crystal growth into a low gravity (g) environment is to reduce or eliminate convective flows. In order to assess the magnitude of the flows at one-g and to confirm their absences at low g a technique is needed to visualize the flow. The Schlieren technique has been previously applied to inorganic crystal growth⁹. It is a logical extension to attempt to apply it to protein crystal growth.

If isothermal crystal growth is considered, there are two parameters which are critical to the application of the Schlieren technique. There must be a change in solution density with a change in concentra-

tion (dp/dc). This change in density will induce flow when a gravitational force is present. In order to image the flow, there must be a change of index or refraction with a change in concentration (dn/dc).

The purpose of this study is to demonstrate the Schlierin effect in different systems, and to measure the dp/dc and dn/dc from these systems to indicate a range of applicability of the Schlierin techniques.

B. Experimental Procedures

The basic Schlierin apparatus has been described in several publications⁹. The apparatus used in these experiments uses a high pressure Xenon arc as a light source. The light is focused onto a 3 ft. focal length spherical mirror which produces a parallel light beam which passes through the crystallization cell. A second spherical mirror followed by a lens system focuses the light onto a knife edge. The Schlieren image is formed on a viewing screen and photographed using a professional quality 16 mm movie camera.

The density of solutions of various concentrations are measured by weighing carefully measured volumes of these solutions on a balance that can weigh to $0.1 \text{ mg} \pm 0.1 \text{ mg}$. The index of refraction is measured using a refractometer thermostated at 20°C . An incandescent light source is used.

The following systems have been studied; Rochelle salt (potassium sodium tartrate), lysozyme, and canavalin. In the Rochelle salt, the solution was saturated at 20°C (380 mg/ml). Growth was induced by lowering the temperature to 5°C . Lysozyme was dissolved in a 0.1 molar sodium acetate solution at a pH of 4.1. The lysozyme concentration was 30 mg/ml. Raising the sodium chloride concentration to 4% w/v caused growth at 19.2°C . In canavalin, protein was dissolved in a solution at pH 9.2 to give a solution concentration of 30 mg/ml. The pH was lowered to 6.7 to induce growth at 19.2°C . All of the growths were done on seed crystals of the respective materials.

C. Results

Schlierin patterns have been seen in all three systems and photographed for the Rochelle salt and lysozyme. Figure 8 is a series of frames from a movie made of the flow in Rochelle salt. The time interval between frames is 1/24 second starting from the top down; the time between each set of frames is 2 seconds. Figure 9 is the same for lysozyme with an interval of 0.8 seconds between frames. The Schlieren work on lysozyme revealed a new factor which significantly influences the kinetics of the protein crystal growth process. This factor was revealed during the growth and dissolution of seed crystals of lysozyme (as evidenced by the flow patterns) which was not consistent with the degree of supersaturation of the growth solution. It was found that if the solution was shaken before the seed crystals were introduced, growth began almost instantaneously. Unshaken solutions exhibited an "incubation" period before a growth plume was formed. In extreme cases, there appeared to be some dissolution of the crystal, as evidenced by a downward going plume before growth began. This effect has been alluded to by Fiddlis, et al.² and Kam and Feher.¹¹

The data on $d\rho/dc$ and dn/dc is shown in Table II.

D. Discussion

This study has shown that Schlierin is applicable to at least some protein systems. The data in Table II, while not complete, indicates that 30 fold differences in dn/dc is no barrier to the application of Schlierin.

While it is expected that there will be no flows in microgravity environments, Schlierin may still have its use in space. Since the technique relies on dn/dc for its imaging ability, it can be used to image the static boundary layers that many develop during low-g growth.

The discovery of a new kinetic factor may lead to a new area of research which may be pursued in the future.

ORIGINAL PAGE IS
OF POOR QUALITY

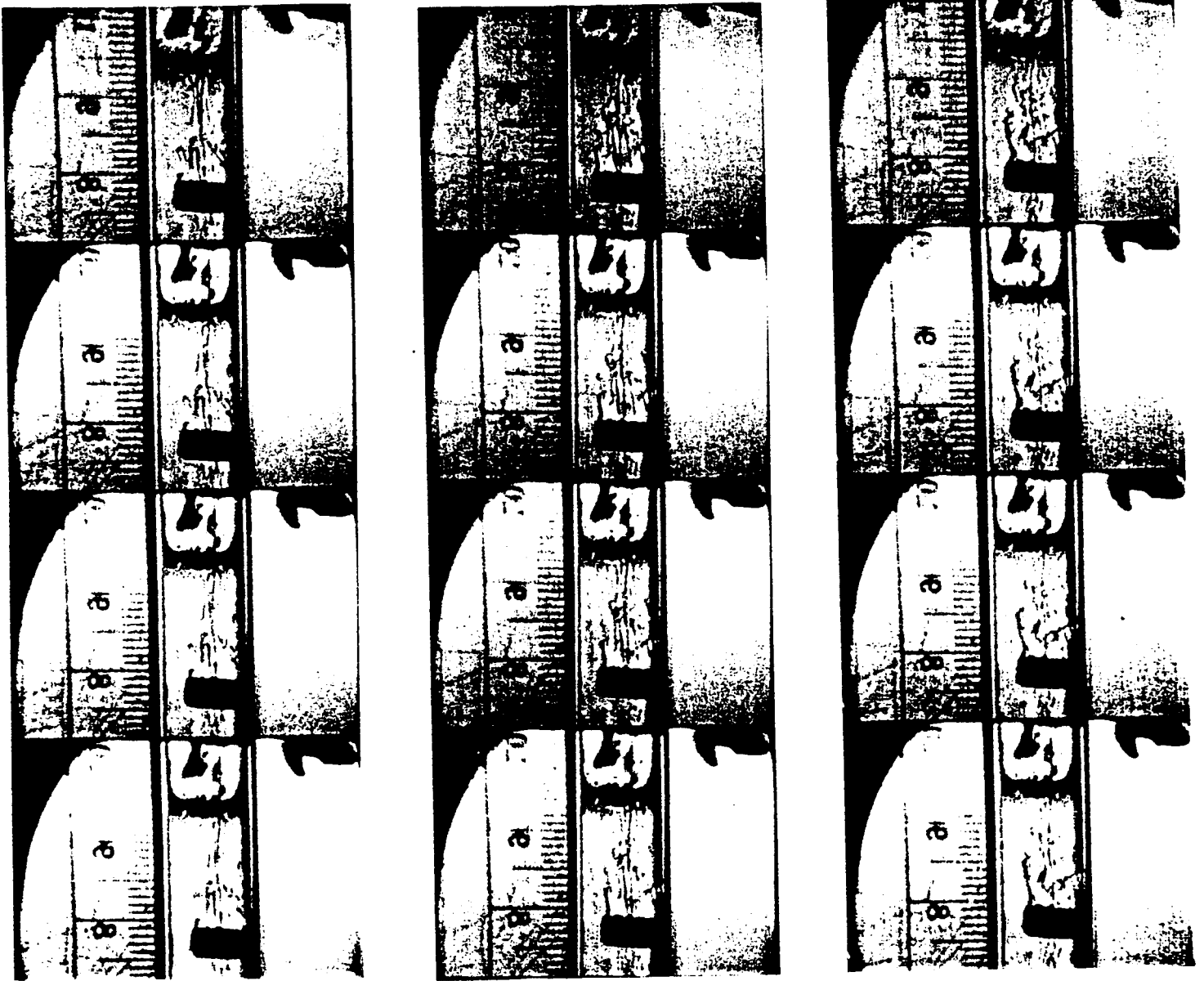


Figure 8: Schlieren photographs of the flows around a growing crystal of Rochelle salt. Time increases from top to bottom of each set at 1/24 second per frame. From left to right each set is 2 seconds apart.

ORIGINAL PAGE IS
OF POOR QUALITY

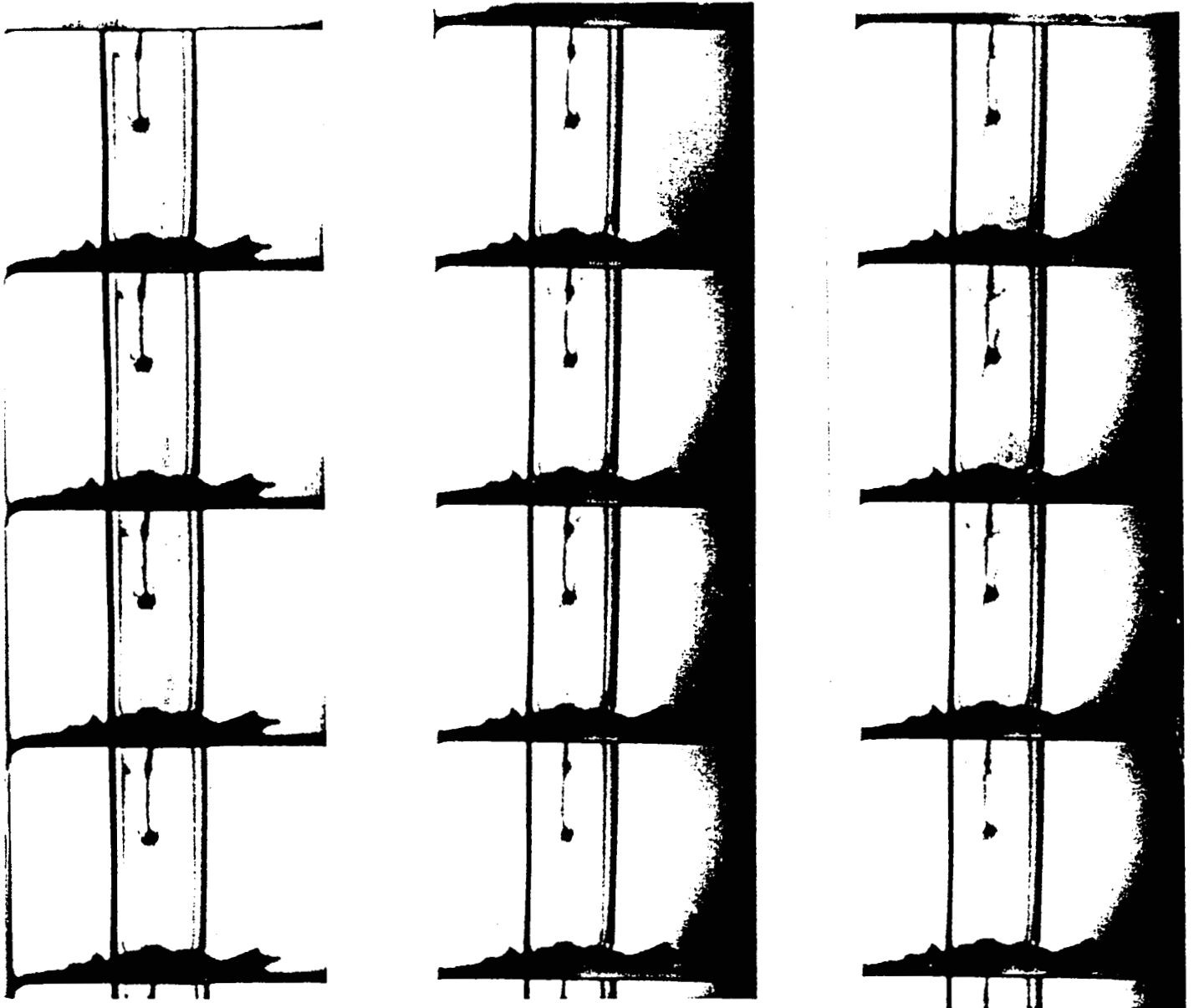


Figure 9: Schlieren photographs of the flows around a growing crystal of lysozyme. Time increases from top to bottom of each set at 0.8 seconds per frame. From left to right each set is 16 seconds apart.

Table 2

Material	Concentration	n	
Water	deionized	1.3305	
Rochelle Salt	231.73 mg/ml	1.3323	
Water + 1% NaCl	+NH ₄ OH to pH 9.2	1.3322	solvent for Canavalin
Canavalin	8.23 mg/ml	1.3344	
Canavalin	12.22 mg/ml	1.3350	
Canavalin	23.31 mg/ml	1.3373	
Canavalin	18.05 mg/ml	1.3386	

for Canavalin $dn/dc = 2.46 \times 10^{-4} \pm .40 \times 10^{-4} \text{ (mg/ml)}^{-1}$

for Rochelle Salt $dn/dc = 7.77 \times 10^{-6} \text{ (mg/ml)}^{-1}$

IV. REFERENCES

1. Mullin, J. W., Crystal Growth Volume 6, edited by B. R. Pamplin, Pergamon Press (1975).
2. Fiddis, R.W., R. A. Longman, and P. D. Calvert, J. Chem. Soc., Faraday Trans. 1, 75:3, 2753.
3. McPherson, A. Jr., Private communication.
4. Pusey, M. and R. Naumann, J. Crystal Growth, 76, 593.
5. Brice, J. C., The Growth of Crystals from Liquids, North Holland (1973).
6. Nielsen, A. E., Kinetics of Precipitation, Pergamon Press (1964).
7. McPherson, A. Jr. and R. Spenser, Arch. of Biochem. and Biophys., 169, 650.
8. Durbin, S. D. and G. Feher, J. Crystal Growth, 76m 583.
9. Chen, P. S., P. J. Shlichta, W. R. Wilcox, and R. A. Lefever, J. Crystal Growth, 47, 43.